Association of Methanol and Water in Ionic Liquids Elucidated by Infrared Spectroscopy Using Two-Dimensional Correlation and Multivariate Curve Resolution

Mercedes López-Pastor,[†,‡] María José Ayora-Cañada,[§] Miguel Valcárcel,[‡] and Bernhard Lendl*[,†]

Institute of Chemical Technologies and Analytics, Vienna University of Technology, Getreidemarkt 9/164AC, A-1060 Wien, Austria, Department of Physical and Analytical Chemistry, University of Jaén, Paraje de las Lagunillas S/N, E-23071 Jaén, Spain, and Department of Analytical Chemistry, University of Córdoba, Campus de Rabanales, Marie Curie Annex Building, E-14071 Córdoba, Spain

Received: December 20, 2005; In Final Form: March 23, 2006

Water and methanol associations in ionic liquids (ILs) have been studied by means of FTIR spectroscopy. Spectra at different concentrations of water or methanol in ILs were obtained by means of on-line dilution using a flow injection analysis system. Spectral features in the OH stretching region revealed that most of the water and methanol molecules tended to be isolated from each other and to interact with the anion of the IL via H bonding. By means of two-dimensional correlation spectroscopy, the formation of methanol and water dimers was also detected. Multivariate curve resolution was used to recover pure spectra and concentration profiles of the different species. Methanol dimers form at concentrations higher than 0.8% (w/w) in the three studied ILs, 1-ethyl-3-methylimidazolium tetrafluoroborate (emimBF_4), 1-butyl-3-methylimidazolium tetrafluoroborate (bmimBF_4), and 1-butyl-3-methylimidazolium hexafluorophosphate (bmimPF_6). Self-association of water molecules takes place in emimBF_4 and bmimBF_4 at a molar ratio similar to that of methanol molecules; however, water dimers cannot be detected in bmimPF_6, the most hydrophobic IL studied. No evidence was found that bigger water clusters are formed in these ILs at the studied cosolvent concentrations.

Introduction

Recently, research has begun on ionic liquid (IL)-based mixed solvents to expand their utility as media for chemical reactions. Several studies indicate that the addition of water and other cosolvents can strongly affect the physical and chemical properties of ILs, such as viscosity,[1,2] electrical conductivity,[3] reactivity,[4] and solvation properties.[5,6] It is important to note that water is also an impurity commonly present in ILs since all known ILs are hygroscopic. Thus, traces of water are thought to be ubiquitous in these materials. For example, ILs containing $[PF_6]^-$ anion are not miscible with water and will readily form a biphasic system with it.[7] However, these ILs (commonly referred to as "hydrophobic") upon prolonged exposure to laboratory air absorb significant amounts of water from the atmosphere.[8,9] Despite the extensive work carried out on applications of ionic liquids, there is still a lack of fundamental knowledge about their structure and physical-chemical properties. In this context, a deeper insight into the interactions between other solvents, such water or methanol, and ILs is needed to better understand the properties of IL-based mixed solvents.

Interactions or molecular states of water and methanol dissolved in various solvents and absorbed in many materials, such as polymers, have been extensively studied using infrared (IR) spectroscopy[10−12] in the OH stretching region (3000−3800 cm^{-1}) since OH stretching vibrations are very sensitive to hydrogen bonding. By contrast, the bending mode of water, which can be found in the region 1595−1650 cm^{-1}, is seldom used to elucidate the molecular state of water, because it hardly changes its position upon hydrogen bonding.

Cammarata et al.[13] studied interactions between ILs and water absorbed from the atmosphere by attenuated total reflectance (ATR) infrared spectroscopy and concluded that anions are responsible for the interaction of ILs and water. No change in band positions and shapes was observed upon increasing the water concentration in the studied range (up to 1.5%, w/w), so it was concluded that only one molecular state of water was present. In addition, they found that in ILs containing $[BF_4]^-$ and $[PF_6]^-$ anions, water forms a symmetric complex (both protons of water bound to two discrete anions): $A^-\cdots H-O-H\cdots A^-$ (where A^- represents the anion in the IL). Tran et al.[14] reported differences in the near-infrared (NIR) spectrum of water dissolved in different ILs, but their study focused on the quantitative determination of absorbed water in ILs rather than on the investigation of its molecular state. On the other hand, Mele et al.[15] studied interactions between the cation and the anion of an IL with water molecules by nuclear magnetic resonance (NMR) spectroscopy. No study about molecular interactions between methanol and ILs has been reported to date.

The goal of this work was to study the behavior of water and methanol dissolved in several 1-alkyl-3-methylimidazolium-based ILs at different cosolvent concentrations to elucidate the possible structure of the interaction water/methanol−IL. To do that, the infrared region of the OH stretching vibrations (3200−3800 cm^{-1}) was analyzed by two-dimensional correlation spectroscopy (2DCoS) and multivariate curve resolution−alternating least squares (MCR−ALS).

* To whom correspondence should be addressed. Fax: +43 1 58801 151 99. E-mail: bernhard.lendl@tuwien.ac.at.
[†] Vienna University of Technology.
[‡] University of Córdoba.
[§] University of Jaén.

10.1021/jp057398b CCC: $33.50
Published on Web 05/13/2006

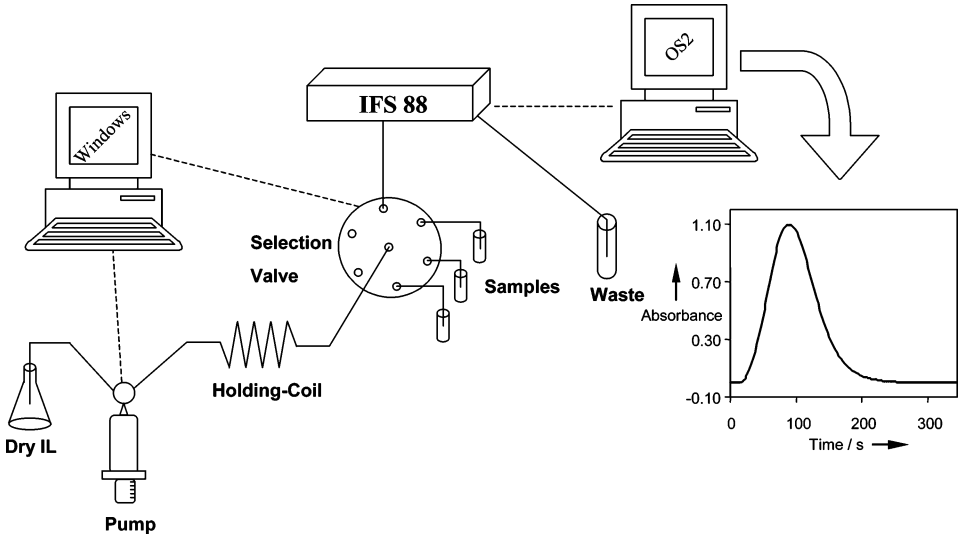

Figure 1. Schematic diagram of the flow injection analysis system showing a typical flow injection profile. Absorbance is shown at 3580 cm^{-1} for methanol/emimBF_4 mixtures retrieved during the flow injection peak.

Experimental Section

Reagents and Instrumentation. All the ionic liquids, 1-ethyl-3-methylimidazolium tetrafluoroborate (emimBF_4), 1-butyl-3-methylimidazolium tetrafluoroborate (bmimBF_4), and 1-butyl-3-methylimidazolium hexafluorophosphate (bmimPF_6), were purchased from Fluka and used as received. To ensure the purity of the ILs, they were characterized by mid-IR. Furthermore, the amount of water in the studied ILs was determined by a Karl Fischer titration through a Karl Fischer titrator, Metrohm 716 DMS Titrino. In this way, the concentration of water encountered in the pure ILs did not exceed 0.1% (w/w) in any case. Methanol (HPLC grade), purchased from Merck, and distilled water were also employed. Standard water/methanol mixtures in the ionic liquids were prepared gravimetrically.

The mid-IR spectra were recorded on an IFS-88 FTIR spectrometer (Bruker, Ettlingen, Germany) equipped with a nitrogen-cooled middle band mercury cadmium telluride (MCT) detector. Spectrum acquisition was carried out at a scanning speed of 100 kHz (HeNe modulation frequency) using Blackmann-Harris three-term apodization and a spectral resolution of 4 cm^{-1}. For each spectrum 32 scans were averaged. A flow cell consisting of CaF_2 windows and a Teflon spacer with a thickness of 25 μm was used.

The flow injection system was set up with a Cavro (Sunnyvale, CA) XP 3000 syringe pump with a syringe of 1000 μL, a holding coil with a capacity of 2000 μL, and a Valco (Houston, TX) six-port selection valve equipped with an electronic microactuator. PTFE tubings (0.50 mm i.d.) were used. All tubings and fittings were obtained from Global FIA (Gig Harbor, WA). The flow system was computer controlled by homemade software (Sagitarius V3), and the FT-IR spectrometer was controlled through OPUS software running on an IBM computer in an OS/2 surrounding.

Procedure. Infrared spectra of ILs containing different amounts of water and methanol were obtained in a fast and reproducible fashion by automated on-line dilution of gravimetrically prepared standard mixtures using the flow injection setup shown in Figure 1. The underlying fundamental process is the generation of a concentration gradient through the reproducible dispersion of a sample injected into an unsegmented carrier stream. Standard mixtures of methanol−IL containing ca. 10% methanol were prepared for all ILs studied. Mixtures containing 6% water were prepared for emimBF_4 and bmimBF_4. For bmimPF_6 a mixture containing 2% water was used due to the poor miscibility of both liquids. Single plugs of the standard mixtures (50 μL) were aspirated into the holding coil (which was previously filled with the corresponding pure ionic liquid). Flow reversal and transport to the detector at a velocity of 50 μL min^{-1} produced a characteristic dispersion pattern which resulted in mixtures of different compositions. Infrared spectra were continuously recorded using the routine LC/GC−IR measurements available within the OPUS software. The background spectrum was recorded with the corresponding pure ionic liquid. In Figure 1 a typical flow injection profile corresponding to methanol dissolved in emimBF_4 is shown. The concentration ranges covered for the different water−IL or methanol−IL mixtures were calculated considering the dispersion in the flow system and are summarized in Table 1.

TABLE 1: Dispersion Coefficient, *D*,[a] and Concentration Range of Cosolvent Dissolved in ILs

	methanol		water	
	D	range (%)	*D*	range (%)
bmimPF6	2.38	0−4.2	3.6	0−0.5
bmimBF4	2.33	0−4.5	2.52	0−2.8
emimBF4	1.66	0−6.0	1.97	0−3.6

[a] D = [Co]/C, where [Co] = concentration of cosolvent in the standard solution and C = concentration at the flow injection peak maximum.

Data Analysis. *Two-Dimensional Correlation Spectroscopy*. 2DCoS performs cross-correlation analysis of a series of spectra of an evolving system that is changed with some master variable, e.g., temperature, time, reaction time, concentration, pH, etc. It spreads the series of one-dimensional spectra into a second spectral dimension, thus yielding two-dimensional maps with the same wavenumber axis in both dimensions. The 2D wavenumber−wavenumber correlation analysis provides two different correlation maps, a synchronous and an asynchronous one. The asynchronous correlation map shows correlations between all spectral bands changing in the experiment and whether they increase or decrease relative to each other. On the other hand, the asynchronous correlation map emphasizes changes occurring at different rates (out-of-phase), and the results are especially useful in discriminating highly overlapping bands, since cross-peaks are observed for different molecules (or even parts of a molecule) as long as they exhibit different

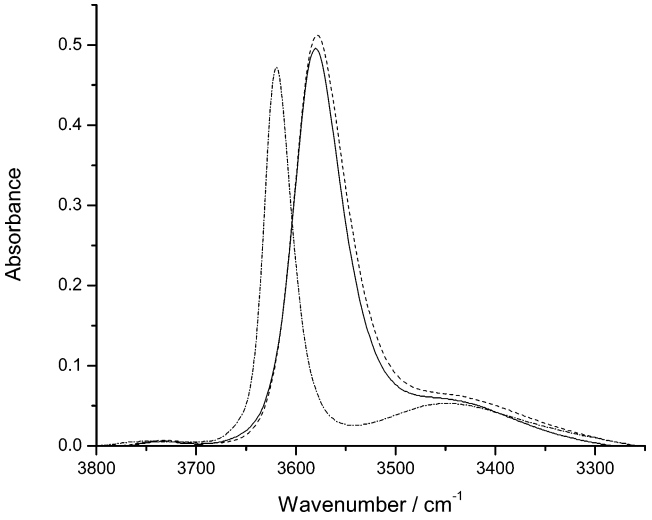

Figure 2. Infrared spectra in the OH stretching regions of ca. 4% w/w methanol solutions in $emimBF_4$ (solid line), $bmimBF_4$ (dashed line), and $bmimPF_6$ (dashed−dotted line).

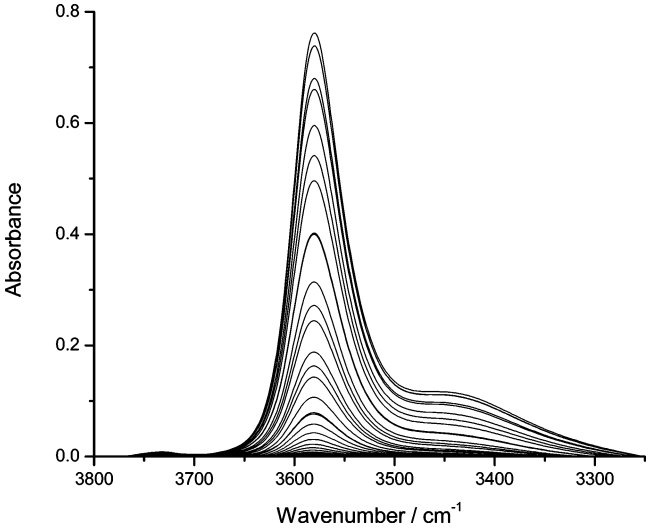

Figure 3. Selected spectra of methanol at different concentrations in $emimBF_4$ in the OH stretching region.

dynamic responses to the applied master variable. 2DCoS can be a powerful tool to study intermolecular interactions such as hydrogen bonding[16,17] and is used here to detect the presence of different associations of molecules dissolved in ILs. If there are different species depending on the cosolvent concentration, the corresponding bands will appear as separate features in the asynchronous maps.

Multivariate Curve Resolution. MCR belongs to a different group of chemometric methods, which have been developed for the components that contribute spectroscopically to the experimentally measured data matrix. In MCR the data set is decomposed into the product of two smaller matrices containing the concentration profiles and the spectra of the modeled components. Thus, quantitative information on the amount of spectral contribution of each component in every spectrum of the data set is obtained. MCR is a very flexible iterative method that allows the inclusion of different chemical constraints and also the simultaneous analysis of several data sets. A useful constraint is nonnegativity of concentrations and spectral intensities. Other constraints may be adapted according to the chemical knowledge available. MCR has already been successfully applied to a broad range of different dynamic systems, including chemical reactions,[18] liquid chromatography,[18,19] and protein folding,[20] among others.

Results and Discussion

Methanol−Ionic Liquid Mixtures. Figure 2 shows selected spectra of ca. 4% methanol solutions in each ionic liquid in the OH stretching region. Methanol dissolved in $emimBF_4$ and $bmimBF_4$ shows nearly identical spectral features, while bands of methanol dissolved in $bmimPF_6$ appear at higher wavenumbers. All the spectra show a sharp band (located at 3580 cm^{-1} for ILs containing $[BF_4]^-$ anion and at 3620 cm^{-1} for $bmimPF_6$) and a broad band of minor intensity centered at about 3440 cm^{-1}. The latter band is not visible at low methanol concentrations (see Figure 3). Spectral changes occurring when the methanol concentration in ILs increases have been analyzed in more detail by 2DCoS and MCR−ALS.

Two-Dimensional Correlation Spectroscopy. The synchronous maps obtained for all ILs (figure not shown) are dominated by one major peak located at 3580 cm^{-1} for $[BF_4]^-$-based ILs and at 3620 cm^{-1} for $bmimPF_6$. These peaks just reflect the increase in methanol concentration but provide no useful information about the presence of different methanol associates.

The asynchronous correlation maps are given in Figure 4. Correlation peaks in the asynchronous map of $bmimPF_6$ can be found at 3440−3620 and 3670−3620 cm^{-1}. This indicates that the band at 3620 cm^{-1} comes from a methanol species different from that of the broad band at 3440 cm^{-1}. Furthermore, a band located at 3600 cm^{-1}, which is not readily observable in the one-dimensional spectra due to overlap with the band at 3620 cm^{-1}, is revealed with the help of the asynchronous correlation map. No correlation peak at 3600−3440 cm^{-1} is observed, which indicates that these two bands correspond to the same methanol species. The weak peak observed at 3670 cm^{-1} does not show asynchronous peaks at 3600 and 3440 cm^{-1}. In this case it is difficult to say if this band corresponds to the same methanol species, or if the absence of the asynchronous peak is just due to the low intensity in the 3670 cm^{-1} region. Correlation peaks in the asynchronous map are coincident for both ILs with $[BF_4]^-$ anion. A broad peak can be found centered at 3430−3580 cm^{-1}, with a shoulder at 3532−3580 cm^{-1}. Again, the band at 3580 cm^{-1} comes from a methanol species different from that of the other bands. The absence of asynchronous peaks between these bands suggests that they belong to the same type of methanol association.

It can be concluded that two different types of methanol associations are present in the studied ILs. The first one shows only one band, located at 3620 cm^{-1} in $bmimPF_6$ and at 3580 cm^{-1} in $[BF_4]^-$-based ILs. The second species shows two major bands at 3600 and 3440 cm^{-1} in $bmimPF_6$ and 3532 and 3430 cm^{-1} in ILs with $[BF_4]^-$. A third low-intensity band at higher wavenumber could also be attributed to this methanol species at 3670 cm^{-1} for $[PF_6]^-$, which, however, was not observed in $[BF_4]^-$-based ionic liquids. Furthermore, it should be noted that the low intensity of the correlation peak for this band makes its assignment difficult.

The coincidence in the spectral features and in the observed correlation maps for ILs containing the same anion but different cations suggests that, as pointed out by Cammarata and coworkers for water dissolved in ILs,[13] the anions play a major role in the interaction with OH moieties.

Multivariate Curve Resolution−Alternating Least Squares. MCR−ALS has been applied to the three data sets to extract pure concentration profiles of the different methanol species present in the ILs. The first step for the analysis of the data

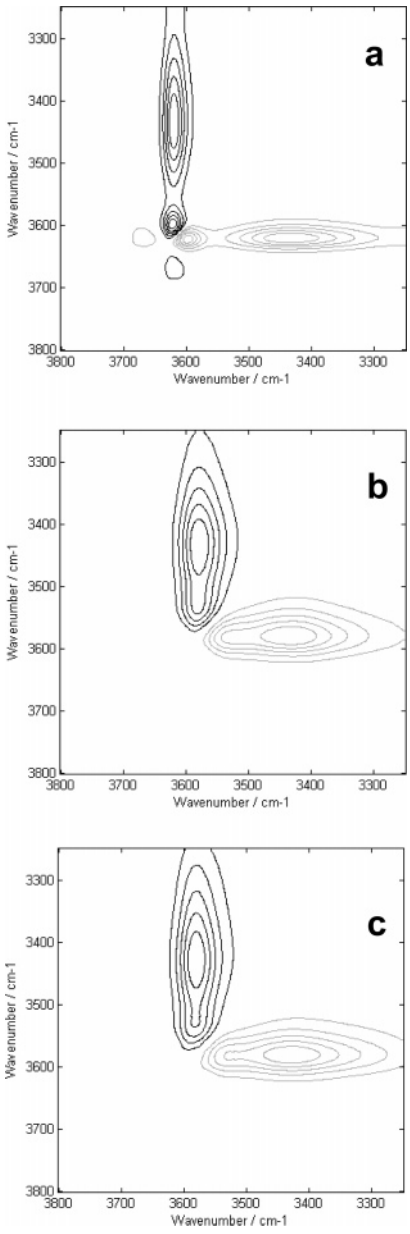

Figure 4. Asynchronous two-dimensional FT-IR correlation maps from concentration-dependent spectral changes of methanol in $bmimPF_6$ (a), $bmimBF_4$ (b), and $emimBF_4$ (c). Positive peaks are shown by gray lines, whereas negative peaks are shown by black lines.

employing MCR consists of the determination of the number of components to be modeled. The number of species was determined by principal component analysis (PCA). The results from PCA allowed the identification of two components, contributing to the explanation of most of the spectral variance of the system (more than 99.99%) in all ILs. These results agree with the observations made using 2DCoS. Results obtained from 2DCoS were used for the identification of pure variables to construct the initial estimates for MCR, as proposed by Jung.[13,21] We took the dominant cross-peak in the asynchronous map and used the intensity profiles of these two bands (3620 and 3440 cm^{-1} for $bmimPF_6$, 3580 and 3430 cm^{-1} for $[BF_4]^-$-based ILs) as initial estimates of the concentration profiles. During optimization, nonnegativity of the spectra and concentration profiles and unimodality of the concentration profiles were applied as constraints. According to 2DCoS, $[BF_4]^-$-based ILs exhibit identical spectral features, and they were therefore analyzed together in a columnwise augmented matrix.

The results of MCR analysis performed in this way are shown in Figure 5. Pure spectra and pure concentration profiles of the two methanol species detected in ILs are obtained. Spectral features of the two components will be discussed later in more detail together with the observations made by 2DCoS. Here, we focus on the retrieved concentration profiles.

All recovered concentration profiles are characterized by the concentration gradient created due to sample dispersion, but interestingly, the shapes of the concentration profiles are very similar for the two ionic liquids containing the cation $[bmim]^+$ and different from those of $emimBF_4$. When a sample is injected in a flow injection system, it forms a dispersed zone, the shape of which depends on the geometry of the channel and the flow velocity. Since the geometry and flow rate were the same for all experiments, the differences in shape must be attributed to the different viscosities of the ILs containing $[bmim]^+$ and $[emim]^+$ cations. Although values found in the literature for absolute viscosities of ILs differ considerably, probably due to inconsistent sample purity,[2] both $[bmim]^+$-based ILs are more viscous than $emimBF_4$. Reported viscosity values[22] for $emimBF_4$ are close to 50 cP, whereas for $[bmim]^+$-based ILs values are in all cases higher than 200 cP. $[bmim]^+$-based ILs show a lower peak height and a greater peak width, which means more dispersion. As has been described in detail during the development of the physical bases of flow injection analysis, dispersion (or mixing) of a sample in a flow injection system is the result of two different phenomena: convection and diffusion.[23] The shape of the observed flow injection peak is dominated by convection, which results from the strong laminar flow profile in the tubings.[24] Increased radial diffusion causes reduced dispersion. Therefore, as the diffusion coefficient is inversely proportional to viscosity, less dispersion is observed for the less viscous ionic liquid.

Furthermore, from the recovered concentration profiles and considering the dispersion of the sample, the concentration at which the second component appears can be estimated. It can be said that for all ILs the second component does not exist at methanol concentrations lower than 1.3% (w/w). Specifically, for $bmimBF_4$ the second component appears at molar ratios of methanol to IL higher than 0.06 (0.85%, w/w), whereas for $emimBF_4$ and $bmimPF_6$ a molar ratio of methanol to IL higher than 0.08 (1.29% and 0.9%, w/w, respectively) is needed.

Methanol Molecular States in Ionic Liquids. Combining the results obtained from 2DCoS and MCR−ALS, the nature of the two different methanol species found can be discussed. The first one (solid line in Figure 5) shows only one band in the OH stretching region, located at 3620 cm^{-1} in $bmimPF_6$ and at 3580 cm^{-1} in $[BF_4]^-$-based ILs. The second species (dashed line in Figure 5) exhibits two features, one broad band (located at 3440 and 3420 cm^{-1} for $bmimPF_6$ and the two $[BF_4]^-$-based ILs, respectively) and one sharp band (at 3600 for $bmimPF_6$ and 3581 cm^{-1} for $[BF_4]^-$-based ILs). Comparing these spectral features with those of methanol diluted in CCl_4,[25] the first species can be assigned to the methanol monomer, which appears in CCl_4 at 3644 cm^{-1}. The red shift observed is due to the interaction of the methanol monomer with the anion of the IL via H bonding. The red shift is larger for ILs containing $[BF_4]^-$, which indicates that $[BF_4]^-$ interacts more strongly with methanol than $[PF_6]^-$ does. For the second species, the broad band could be attributed to the donor OH group of a hydrogen-bonded methanol open dimer (observed experimentally at 3517 cm^{-1} in CCl_4), whereas the sharp band corresponds to the acceptor OH group (not observed experimentally by Dixon et al.[25] due to the overlap with the monomer band), still interacting

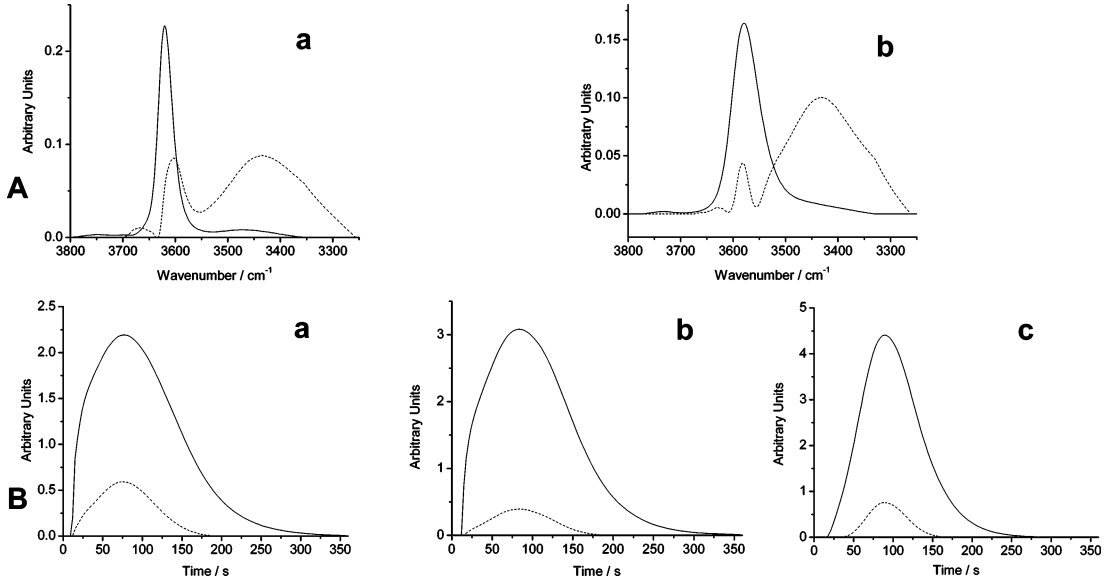

Figure 5. Results of analysis performed by multivariate curve resolution of studied ionic liquids: (A) spectra of methanol species in bmimPF_6 (a) and in $[BF_4]^-$-based ionic liquids (b); (B) concentration profiles in bmimPF_6 (a), bmimBF_4 (b), and emimBF_4 (c); first component (solid line), second component (dashed line).

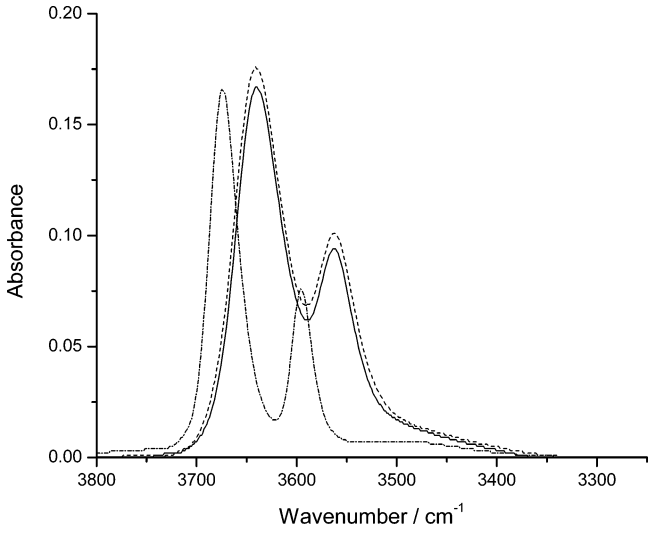

Figure 6. Infrared spectra in the OH stretching regions of ca. 0.35% (w/w) water solutions in emimBF_4 (solid line), bmimBF_4 (dashed line), and bmimPF_6 (dashed−dotted line).

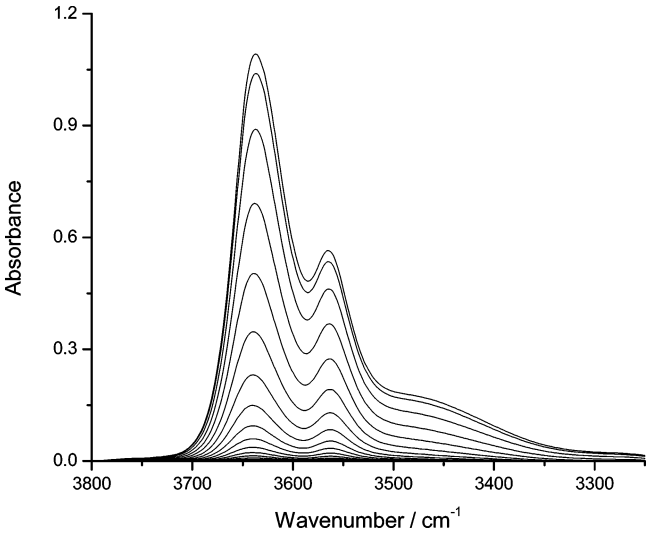

Figure 7. Selected spectra of water at different concentrations in emimBF_4 in the OH stretching region.

with the anion of the IL. The weak feature present at 3670 cm^{-1} in bmimPF_6 was observed by Dixon et al. too. They attributed this weak band to the combination between the OH stretching mode and a low-frequency motion. Our findings agree well with previous theoretical studies of methanol dissolved in CCl_4. According to Staib,[26] the calculated IR spectrum of the monomer exhibits a unique band at 3663 cm^{-1} (experimental value 3644 cm^{-1}, ref 29), whereas the methanol open dimer in CCl_4 shows two bands located at 3640 cm^{-1} (sharp) and 3500 cm^{-1} (broad). The difference in the maximum positions of the two bands in the methanol dimer is 140 cm^{-1} for the calculated spectrum in CCl_4, 160 cm^{-1} for methanol dissolved in bmimPF_6, and 161 cm^{-1} for ILs containing $[BF_4]^-$. It can be therefore concluded that the second species of methanol detected in ILs corresponds to an open dimer, which is formed at methanol concentrations higher than 1.3% (w/w).

Water−Ionic Liquid Mixtures. Figure 6 shows selected spectra at ca. 0.35% (w/w) water in each ionic liquid at the OH stretching region (3250−3800 cm^{-1}). As happened for methanol, the spectra of water dissolved in emimBF_4 and bmimBF_4 are nearly identical, while bands of water dissolved in bmimPF_6 appear at higher wavenumbers. According to Cammarata et al.,[13] the two narrow, well-separated bands observed at ca. 3650 and 3570 cm^{-1} can be assigned to the antisymmetric (ν_3) and symmetric (ν_1) stretch vibrations of the water monomer, which exists in ILs forming symmetric 1:2-type H-bonded complexes, anion−HOH−anion.

Figure 7 plots spectra at different water concentrations in ionic liquids obtained with the described flow injection system. The $[BF_4]^-$-based ILs can dissolve higher amounts of water than the $[PF_6]^-$-based ionic liquid. Visual inspection of these spectra shows that ν_1 and ν_3 stretching modes begin to overlap in $[BF_4]^-$-based ILs while no overlapping can be observed in the $[PF_6]^-$-based ionic liquid. Furthermore, overlapping is higher in emimBF_4 than in bmimBF_4.

Two-Dimensional Correlation Spectroscopy. The synchronous maps obtained for $[BF_4]^-$-based ILs (not shown) are dominated by two major peaks located at 3637 and 3563 cm^{-1} and a minor one at 3450 cm^{-1}. Two peaks have been obtained for bmimPF_6 at 3675 and 3595 cm^{-1}. These peaks reflect the

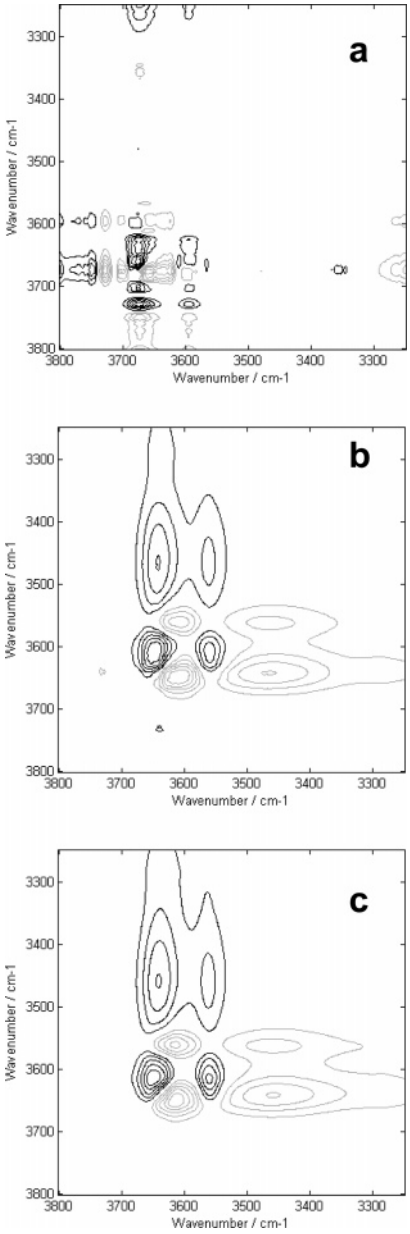

Figure 8. Asynchronous two-dimensional FT-IR correlation spectra from concentration-dependent spectral changes of water in $bmimPF_6$ (a), $bmimBF_4$ (b), and $emimBF_4$ (c). Positive peaks are shown by gray lines, whereas negative peaks are shown by black lines.

increase in water concentration. The corresponding asynchronous correlation maps are given in Figure 8. Correlation peaks in the asynchronous map are coincident for both ILs with $[BF_4]^-$ anion. Peaks can be found at 3640−3610, 3560−3610, 3640−3450, and 3560−3450 cm^{-1}. The asynchronous map from $bmimPF_6$ is very noisy. Although correlation peaks can be found at 3675−3650, 3595−3650, 3675−3480, and 3595−3480 cm^{-1}, their intensity is comparable to noise and thus regarded as not significant. No correlation peaks are found either at 3610−3450 and 3640−3565 cm^{-1} for $[BF_4]^-$-based ILs or at 3650−3480 and 3675−3595 cm^{-1} for $bmimPF_6$, which demonstrates that each pair of bands belong to the same water species. It can be clearly concluded that two different types of water are present in the studied systems. The first one shows bands at 3640 and 3565 cm^{-1} for $[BF_4]^-$-based ILs and 3675 and 3595 cm^{-1} for $bmimPF_6$. The second water species can only be clearly detected in $[BF_4]^-$-based ILs at the asymmetric correlation band at 3610 and 3450 cm^{-1}.

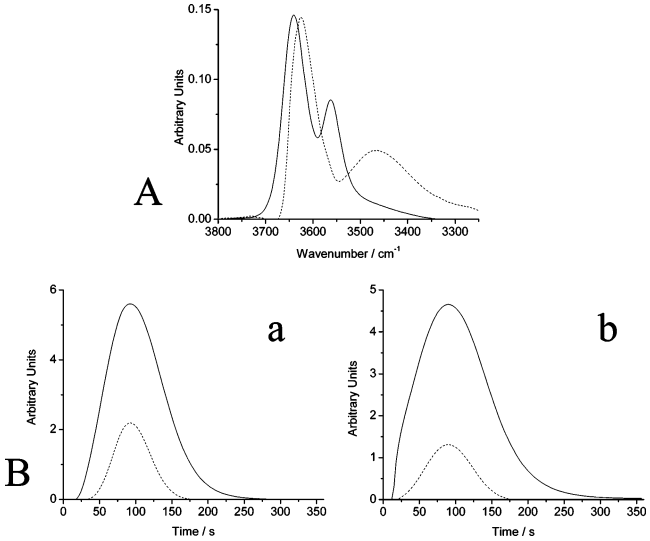

Figure 9. Results of analysis performed by multivariate curve resolution of $[BF_4]^-$-based ionic liquids: (A) spectra of water species in $[BF_4]^-$; (B) concentration profiles in $emimBF_4$ (a) and $bmimBF_4$ (b).

Multivariate Curve Resolution−Alternating Least Squares. The number of components contributing to the explanation of the variability of the system determined by PCA was two for $[BF_4]^-$-based ILs and only one in the case of $bmimPF_6$. These results agree with the observations made using 2DCoS. To construct the initial estimates for developing MCR, the intensity profiles of the bands at 3640 and 3440 cm^{-1} (which give a cross-peak in the asynchronous map) were used. During optimization, nonnegativity of the spectra and concentration profiles and unimodality of the concentration profiles were applied as constraints. For $bmimPF_6$ the data could be fitted using only one component (figure not shown). Again, the two experiments involving $[BF_4]^-$ ILs were analyzed together. The results of the analysis of the data using MCR in this way are shown in Figure 9. The resolved concentration profiles show for both components the typical shape of the flow injection peaks, already discussed for methanol. The component with bands at 3610 and 3450 cm^{-1} (dashed line) does not exist below a molar ratio of water to IL of 0.07 (0.56%, w/w) for $bmimBF_4$ and 0.04 (0.36%, w/w) for $emimBF_4$.

Water Molecular States in Ionic Liquids. The unique kind of water present in $bmimPF_6$ and the first kind of water in the two hydrophilic ILs (solid line in Figure 9) correspond to monomeric water bonded symmetrically with two anions of the IL in a 1:2 complex. In the hydrophobic ionic liquid the measured antisymmetric and symmetric stretch vibrations of the water are less red shifted because the interactions are weaker and the water monomers are only attached to the IL anions without disturbing the IL network. In all cases, in these water molecules, present as monomers bridging two anions, the two H atoms are equivalent and the antisymmetric and symmetric stretching bands of the water molecule are well resolved. This conclusion agrees with the results reported by Cammarata et al.[13] Nevertheless, the second type of water found here in hydrophilic ILs at higher water concentrations was not observed in the above-mentioned study for $bmimBF_4$. The recovered pure spectrum of this second type of water (dashed line in Figure 9) shows a band at 3610 cm^{-1}, which can be attributed to OH interacting with the anion of the IL, but it also shows a broad band shifted to low wavenumber (ca. 3450 cm^{-1}) which indicates the presence of water molecules interacting with each other. The position of the latter band is considerably lower than

that attributed by Köddermann[27] to the water dimer (3553 cm^{-1}) but higher than that of the cyclic water trimer (3409 cm^{-1}) in CCl_4. Considering the general tendency of all stretching bands observed in this study to be red shifted with respect to the bands in CCl_4, it can be concluded that the second water species must be a water dimer, interacting with $[BF_4]^-$ anions. Open water dimers are reported to be more stable than cyclic configurations in the vapor phase[28] and hydrophobic solvents.[25] In the hydrogen bond acceptor unit of the open water dimer the two H atoms are equivalent, whereas in the donor unit they are not. Thus, the open water dimer should show four fundamental transitions in the OH stretching region, the antisymmetric (ν_3) and symmetric (ν_1) stretch vibrations of the proton donor molecule. Three of these absorption bands have been observed in molecular beam experiments.[29] Nevertheless, the recovered spectrum of the second water species observed here shows only two bands. Our observations suggest the existence of a cyclic water dimer, in which each water molecule interacts with an anion of the ionic liquid and another water molecule. The two H atoms are bonded to the anion of the ionic liquid and another water molecule. The two H atoms bonded to the anion of the ionic liquid give rise to the OH stretching band at ca. 3610 cm^{-1}, whereas the two H atoms involved in water−water interactions give the broad absorption band at 3450 cm^{-1} due to the ring stretches as has been described for larger cyclic water clusters ($n = 3-5$).[27,29] Such a cyclic structure could be stabilized due to the interactions with the ions of the IL.

Conclusions

Two different types of water species are found in hydrophilic ILs, while a unique type of water is found in the hydrophobic IL in the studied concentration range. Methanol in two different molecular states is found in all ionic liquids. Water or methanol monomers are still the dominant species at the highest concentrations studied. At about 0.4% and 1% (w/w) concentration of cosolvent water−water and methanol−methanol interactions are observed, respectively. The spectral features of these associates were first identified by means of 2DCoS and then their pure spectra and concentration profiles recovered with the help of MCR. According to the spectral features observed and taking into account previous theoretical and experimental studies, it can be concluded that water and methanol dimers are formed in the IL within the studied concentration range but not larger aggregates. Furthermore, spectral features of methanol/water dissolved in ILs containing the same anion are coincident, which indicates that the interaction of the water/methanol molecules with the ILs via H bonding occurs between the OH groups and the anion of the ILs. In this study the influence of the cation on the properties of the ILs can be seen in the different flow profiles obtained. Dispersion of water and methanol is higher in $[bmim]^+$-based ILs due to their higher viscosity. Furthermore, the cation also influences the molar ratio of cosolvent at which self-association of water and methanol begins. This fact indicates that the cation interacts with water and methanol too, although this interaction is not reflected in spectral changes in the OH region.

Acknowledgment. M.L.P. and M.J.A.C. thank the Spanish Ministry of Education and Science for a predoctoral fellowship and a mobility grant, respectively. Furthermore, we thank Prof. Marcelo Blanco from the University of Barcelona for Karl Fischer studies that were carried out by his group. M.L.P. also acknowledges having received a Marie Curie fellowship (contract: HPMT-CT-2000-00059) for stay at the MC Training site ADVIS.

References and Notes

(1) Wang, J.; Pei, Y.; Zhao, Y.; Hu, Z. *Green Chem.* **2005**, *7*, 196.
(2) Widegren, J. A.; Laesecke, A.; Magee, J. W. *Chem. Commun.* **2005**, 1610.
(3) Widegren, J. A.; Saurer, E. M.; Marsh, K. N.; Magee, J. W. *J. Chem. Thermodyn.* **2005**, *37*, 569.
(4) Brown, R. A.; Pollet, P.; McKoon, E.; Eckert, C. A.; Liotta, C. L.; Jessop, P. G. *J. Am. Chem. Soc.* **2001**, *123*, 1254.
(5) Chakrabarty, D.; Chakrabarty, A.; Seth, D.; Sarkar, N. *J. Phys. Chem. A* **2005**, *109*, 1764.
(6) Mancini, P. M.; Fortunato, G. G.; Vottero, L. R. *Phys. Chem. Liq.* **2004**, *42*, 625.
(7) Anthony, J. L.; Maginn, E. J.; Brennecke, J. F. *J. Phys. Chem. B* **2001**, *105*, 10942.
(8) Huddleston, J. G.; Visser, A. E.; Reichert, W. M.; Willauer, H. D.; Broker, G. A.; Rogers, R. D. *Green Chem.* **2005**, *3*, 156.
(9) Seddon, K. R.; Stark, A.; Torres, M. J. *Pure Appl. Chem.* **2000**, *72*, 2275.
(10) Rudberg, J.; Foster, M. *J. Phys. Chem. B* **2004**, *108*, 18311.
(11) Zoidis, E.; Yarwood, J. *J. Mol. Liq.* **1995**, *64*, 197.
(12) Scherer, J. R. *Advances in Infrared Raman Spectroscopy*; Heyden: London, 1978.
(13) Cammarata, L.; Kazarian, S. G.; Salter, P. A.; Welton, T. *Phys. Chem. Chem. Phys.* **2001**, *3*, 5192.
(14) Tran, C. D.; De Paoli Lacerda, S. H.; Oliveira, D. *Appl. Spectrosc.* **2003**, *57*, 152.
(15) Mele, A.; Tran, C. D.; De Paoli Lacerda, S. H. *Angew. Chem., Int. Ed.* **2003**, *42*, 4364.
(16) Czarnecki, M. A.; Wojtków, D. *J. Phys. Chem. A* **2004**, *108*, 2411.
(17) Segtnan, V. H.; Sasic, S.; Isaksson, T.; Ozaki, Y. *Anal. Chem.* **2001**, *73*, 3153.
(18) Jaumot, J.; Marchan, V.; Gargallo, R.; Grandas, A.; Tauler, R. *Anal. Chem.* **2004**, *76*, 7094.
(19) Salau, J. S.; Honing, M.; Tauler, R.; Barceló, D. *J. Chromatogr., A* **1998**, *795*, 3.
(20) Navea, S.; de Juan, A.; Tauler, R. *Anal. Chem.* **2002**, *74*, 6031.
(21) Jung, Y. M.; Kim, S. B.; Noda, I. *Appl. Spectrosc.* **2003**, *57*, 1376.
(22) Huddleston, J. G.; Visser, A. E.; Reichert, W. M.; Willauer, H. D.; Broker, G. A.; Rogers, R. D. *Green Chem.* **2001**, *3*, 156.
(23) Ruzicka, J.; Hansen, E. H. *Flow Injection Analysis*, 2nd ed.; Wiley: New York, 1988.
(24) Vanderslice, J. T.; Rosenfeld, A. G.; Beecher, G. R. *Anal. Chim. Acta* **1986**, *179*, 119.
(25) Dixon, J. R.; George, W. O.; Hossain, M. F.; Lewis, R.; Price, J. M. *J. Chem. Soc., Faraday Trans.* **1997**, *93*, 3611.
(26) Staib, A. *J. Chem. Phys.* **1998**, *108*, 4554.
(27) Ködermann, T.; Schulte, F.; Huelsekopf, M.; Ludwig, R. *Angew. Chem., Int. Ed.* **2003**, *42*, 4904.
(28) Dyke, T. R.; Muenter, J. S. *J. Chem. Phys.* **1972**, *57*, 5011.
(29) Huisken, F.; Kaloudis, M.; Kulcke, A. *J. Chem. Phys.* **1996**, *104*, 17.